

BACKSCATTERING COEFFICIENTS OF ELECTRONS: A REVIEW

Tatsuo Tabata

*Osaka Prefecture University
1-1 Gakuen-cho, Naka-ku, Sakai, Osaka 599-8531, Japan
and
Institute for Data Evaluation and Analysis
198-51 Kami, Nishi-ku, Sakai, Osaka 593-8311, Japan
Email: ttabata@pearl.ocn.ne.jp*

Abstract

The experiment on the backscattering coefficient of electrons of energies from 3.2 to 14 MeV, published in 1967 by the present author, is reviewed to confirm the usefulness of its results as a benchmark for Monte Carlo calculations. The cause of large discrepancies between Dressel's and other results is described. Comparisons of compiled experimental data and results of Integrated TIGER Series Monte Carlo Code System are cited and discussed. In Appendix, experimental data of the present author's group on the charge deposition profile of electrons are mentioned as another useful benchmark.

1. Introduction

Experimental data on the backscattering coefficient of electrons are useful as a benchmark for Monte Carlo codes for electron-photon transport calculations. In this paper a review is first given of one of the best experiments in the MeV region, published by the present author [1] in 1967, mainly from the viewpoint of the experimental method and evaluation of errors. Secondly the cause of large discrepancies between Dressel's [2] and other authors' results, the latter including the present author's, is mentioned, because it has not been well documented yet. Thirdly graphical comparisons of compiled experimental data and results of Integrated TIGER Series (ITS) Monte Carlo Code System [3] are cited from a previous publication [4] and discussed. In Appendix another useful benchmark on the charge deposition profile of electrons [5, 6] and its comparison with the old version of ETRAN and ITS are reviewed.

2. Present Author's Experiment

2.1. Method

2.1.1. Electron Beam

The linear electron accelerator of the former Radiation Center of Osaka Prefecture (see¹ Fig. 1) produced the electron beams of energies from 3.2 to 14 MeV. An analyzing magnet deflected the beam by 70 deg. A pair of quadrupole magnets focused the beam on the entrance collimator of the scattering chamber placed 5.5 m away in an experimental room. The collimator was made of copper and was 160 mm in length, allowing self-absorption of bremsstrahlung generated near its entrance hole. The energy scale of the analyzing magnet was calibrated within an error of 1.1 % by measuring the conversion-electron line of Cs¹³⁷ and the threshold of the Cu⁶³ (γ , n) reaction.

¹ This and the other figures related to this experiment are those not used in the original paper [1].

2.1.2. Scattering Chamber

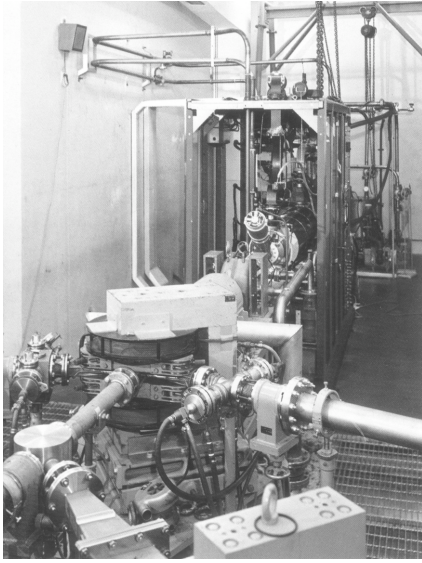


Figure 1. Linear electron accelerator (in the backward) and analyzing magnet (at the center). The analyzed electron beam goes into an experimental room through the pipe on the right. In the forward an energy-monitor system (not used in the experiment described here) is seen.

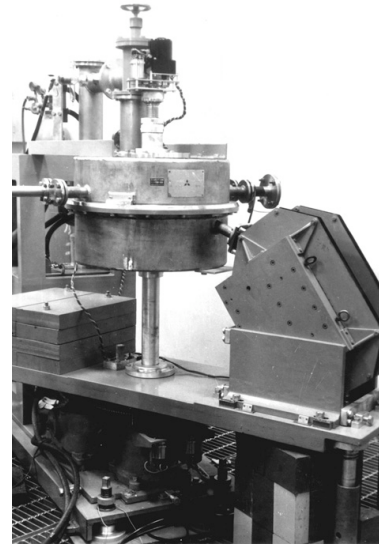


Figure 2. Scattering chamber. The electron beam comes into the chamber from left. The magnet on the right was not used in the experiment described here.

The scattering chamber consisted of a fixed lid and a cylindrical box, each 50 cm i.d. and 15 cm high and made of stainless steel. The measuring port is attached to the box with a dip of 20 deg from the horizontal plane. The box could be rotated by remote control of a drive motor under the preservation of the vacuum of the scattering chamber. The angular position θ_0 of the measuring port in the horizontal plane was indicated to 0.2 deg at the control panel. The scattering angle θ is given by:

$$\cos\theta = \cos(20 \text{ deg}) \cos\theta_0 \quad (1)$$

The vacuum in the scattering chamber was of the order of 10^{-3} Pa. After passing through a detector collimator and through a 3.5-mg/cm² Mylar window in the measuring port, the backscattered electrons entered an ionization chamber. The detector collimator was made of copper and had a conical taper matching the solid-angle cone subtended at the center of the target surface.

2.1.3. Targets and Target Assembly

The target was mounted on the supporting rod with a ring-shaped copper holder and a ceramic insulator, being placed perpendicular to the beam with the center of the incident surface at the center of the scattering chamber. When it was thinner than the maximum range of incident electrons (to measure the dependence of the backscattering coefficient on thickness), the target was backed with an aluminum Faraday cup having an entrance hole 11 mm in diameter and 35 mm in depth, as shown in Fig. 3. All the targets were of purity better than 99.5 %.

2.1.4. Ionization Chamber and Measurement

The ionization chamber was of the X-ray compensation type developed by Van de Graaff *et al.* [7]. The charge collector was an aluminum plate 60 mm in diameter and 30 mm thick, sandwiched between two sheets of aluminum foil 27 mg/cm² thick. The gap between the charge collector and each of the sheets was about 4 mm, being filled with air at atmospheric pressure. High voltages of opposite polarities applied to the foils reduced X-ray background.

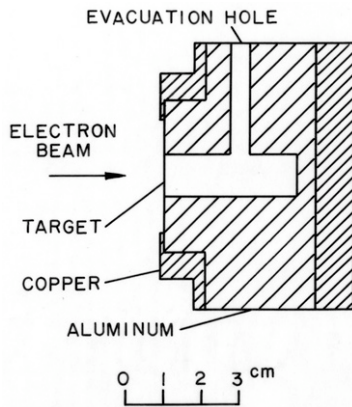


Figure 3. Target assembly for measuring dependence of backscattering coefficient on absorber thickness.

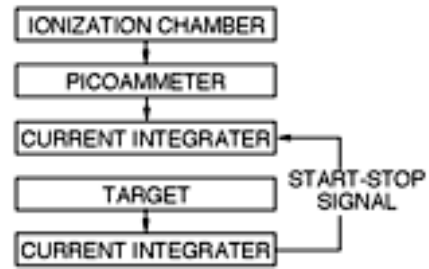


Figure 4. Block diagram of measurement.

A block diagram of measurement is given in Fig. 4. The current from the ionization chamber was amplified with a picoammeter and fed to a current integrator, while the target current was measured with another current integrator. The signal from the latter integrator controlled the simultaneous start and stop of measurement with the former integrator.

The multiplication factor f of the ionization chamber depends on the energy spectrum of backscattered electrons, but a simple assumption was made that it was determined as a function of average energy $E_{av}(E_0, Z)$ of backscattered electrons from the effectively semi-infinite target, where E_0 is the incident electron energy and Z is the atomic number of the target material. Values of $E_{av}(E_0, Z)$ were estimated by interpolation and extrapolation of the experimental results of Wright and Trump [8].

On the above assumption, the calibration of f was made from the ratio of fI_b obtained with the ionization chamber to I_b measured with a Faraday chamber for the absorber of a thick gold target. The Faraday chamber consisted of a brass chamber in which an aluminum collector of 60 mm in diameter and 30 mm thick was contained, and it was directly attached to the measuring port of the scattering chamber. A correction of Faraday chamber efficiency for backscattering and secondary emission from the collector was made, and ranged from 4.1 to 8.9 %.

2.1.5. Background

The X-ray background uncompensated in the ionization chamber was measured under each condition by closing a remotely controlled shutter in front of the ionization chamber. The shutter consisted of a copper plate 40 mm in diameter and 10 cm thick, and could prevent electrons from entering the ionization chamber. Smaller background of another type, mainly due to secondary electrons produced near the measuring port of the scattering chamber by bremsstrahlung X rays from the entrance collimator, was studied for each incident energy without the target. The total background was always highest at 160 deg where the ratio of background to signal was about 0.5–20 % depending on E_0 and Z .

When the Faraday chamber was used for calibration, the background was measured by inserting an aluminum plug 35 mm long in the detector collimator. The ratio of background to signal at 160 deg increased from 2 to 12 % with increasing energy.

2.1.6. Secondary Electrons

Values of the secondary emission coefficient δ were necessary for the correction of the target current I_t . These were measured with the aid of a ring-shaped electrode attached to the incident side of the target.

2.2. Errors

Possible sources of systematic errors and their values were as follows:

- (1) The multiplication factor f of the ionization chamber, ± 2.9 –8.1 % depending on E_0 and Z .
- (2) The solid angle of detection, $\pm 1.8\%$.
- (3) The secondary emission coefficient δ (due to the possible change of surface condition during bombardment with electron beams), $\pm 10\%$.

(4) The ionization chamber current $I_i(\theta)$ (due to a possible unmeasured background), $\pm 1\%$.

(5) The target current I_t (due to secondary emission from the target caused by bremsstrahlung, and re-backscattering of electrons from the walls of the scattering chamber to the target), $\pm 0.5\%$.

(6) The ratio $I_i(\theta)$ (due to the relative accuracy of the picoammeter and the current integrator), $\pm 1.5\%$.

Total errors in backscattering coefficients were 6.7–14 % depending on E_0 and Z , as shown in Tables I and II of the original paper [1]. The present review, made after forty years since the publication of the paper, has found no problems either in the experimental method or in the evaluation of errors. The backscattering coefficients obtained are shown in Figs. 5 and 6 by solid symbols.

Figure 5. Comparison of compiled experimental backscattering coefficients of electrons for Be, C and Al targets with ITS Monte Carlo results (cited from Ref. 4 with changes in symbols). Solid symbols show present author's experimental results [1].

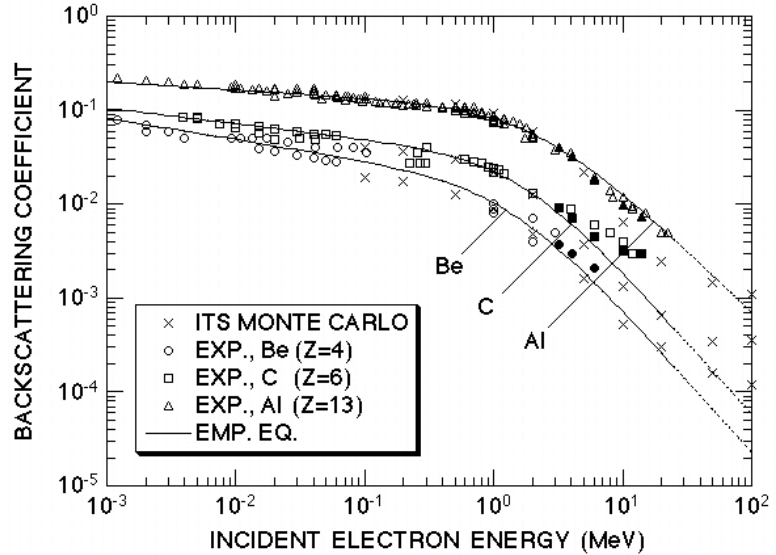
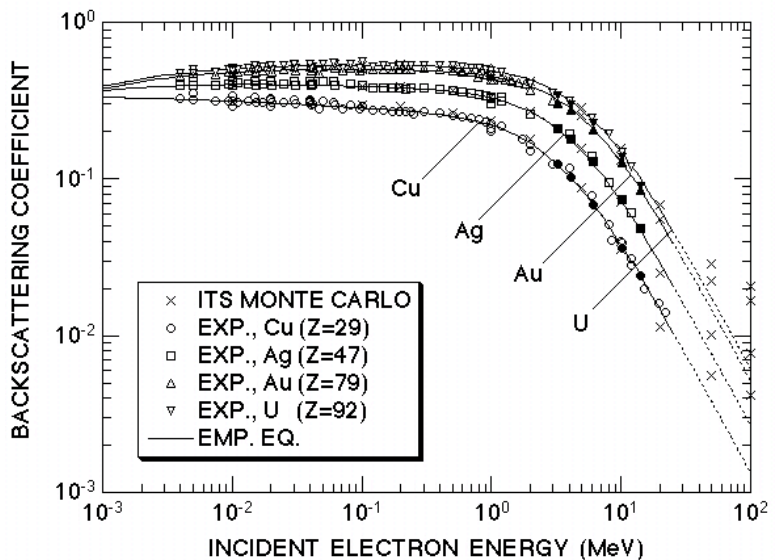


Figure 6. Comparison of compiled experimental backscattering coefficients of electrons for Cu, Ag, Au and U targets with ITS Monte Carlo results (cited from Ref. 4 with changes in symbols). Solid symbols show present author's experimental results [1].



3. Cause of Discrepancies between Dressel's and Other Results

A little before the publication of the present author's experimental results, Dressel [2] reported the backscattering coefficients measured in the energy region from 0.5 to 10 MeV, and these were appreciably higher than previous authors' results. On the other hand, the present author's results were in agreement or consistent with the previous authors'. Therefore, the present author wrote in his paper [1] about possible causes of errors in Dressel's experiment. Among the four items written, the first one, i.e., the efficiency of the beam current monitor, had been rather close to the actual cause found later by Dressel [9], but had not been an entirely correct guess.

In Dressel's experiment, the electron beam was monitored by a pickup loop [10], which received an induced voltage pulse for each passage of an electron bunch. This monitor was placed at the upstream side of the last-stage collimator, which was located at the entrance of the scattering chamber. The diameter of the main beam was smaller than the hole of the collimator, but an unnoticed peripheral halo of electrons, which issued from collimators, was accompanying the main beam. While most of the halo electrons were incident on the target, the forward exit port of the scattering chamber, to which a Faraday cup was connected for calibrating the monitor, was too narrow to make all the halo electrons to pass through. Thus the number of electrons actually incident on the target was much larger than indicated by the monitor. Dressel did not notice the halo electrons earlier because of the following reason: These electrons had a broad distribution with a few percent of the current density of the main beam, and this density was below the background of his beam profile measurement, in which he used photographic film and Plexiglas.

4. Comparison of Experimental Data with ITS Monte Carlo Results

In 1971 the present author's group compiled experimental data on the backscattering coefficient of electrons, and made an empirical equation fitted to these [11]. Later they published a modified equation on the basis of an extended compilation [4, 12, 13], with which comparison was made of the Monte Carlo results (numerical data are given in Ref. 12) generated by ITS [3]. Figures 5 and 6, which show the comparison, have been taken from Ref. 4 with some changes in symbols. It can be seen that the ITS results agree rather well with experimental data except when the backscattering coefficient is considerably small, i.e., at 5 MeV for Be, at 10 MeV for C and at 10 and 20 MeV for Al (see Fig. 5). Another feature seen from these figures is this: Experimental data for Be, C and Al, as well as the ITS results for all absorbers studied, have the trend that the coefficient decreases slower than indicated by the empirical equation at high energies.

References

- 1) T. Tabata, Phys. Rev. **162**, 336 (1967).
- 2) R. W. Dressel, Phys. Rev. **144**, 332 (1966).
- 3) J. A. Halbleib, R. P. Kensek, T. A. Melhorn, G. Valdez, S. M. Seltzer and M. J. Berger, ITS Version 3.0: The Integrated TIGER Series of Coupled Electron/Photon Monte Carlo Transport Codes, Report SAND91-1634, Sandia Nat. Labs. (1992).
- 4) R. Ito, P. Andreo and T. Tabata, Radiat. Phys. Chem. **42**, 761 (1993).
- 5) T. Tabata, R. Ito, S. Okabe and Y. Fujita, Phys. Rev. B **3**, 572 (1971).
- 6) T. Tabata, P. Andreo, K. Shinoda and R. Ito, Nucl. Instr. Methods B **95**, 289 (1995).
- 7) R. J. Van de Graaff, W. W. Buechner and H. Feshbach, Phys. Rev. **69**, 452 (1955).
- 8) K. A. Wright and J. G. Trump, J. Appl. Phys. **33**, 687 (1962).
- 9) R. W. Dressel, Private communication (1968).
- 10) R. W. Dressel, Nucl. Instr. Methods **24**, 61 (1963).
- 11) T. Tabata, R. Ito and S. Okabe, Nucl. Instr. Methods **94**, 509 (1971).
- 12) R. Ito, P. Andreo, and T. Tabata, Bull. Univ. Osaka Pref. **41**, No. 2, 69 (1993).
- 13) T. Tabata, P. Andreo and K. Shinoda, Radiat. Phys. Chem. **54**, 11 (1999).
- 14) D. W. O. Rogers, Health Phys. **46**, 891 (1984).
- 15) P. Andreo and A. Brahme, Radiat. Res. **100**, 16 (1984).
- 16) D. W. O. Rogers and A. F. Bielajew, Trans. Am. Nucl. Soc. **52**, 380 (1986).
- 17) T. Tabata, P. Andreo and R. Ito, Nucl. Instr. Methods B **94**, 103 (1994).

Appendix

In this Appendix, the charge deposition profiles measured by the present author's group [5] are mentioned as another useful benchmark for Monte Carlo calculations. They used the same experimental system as described in Sec. 2 to measure the depth profiles of charge deposition in elemental materials produced by electrons of energies from 4.09 to 23.5 MeV (measurements at the highest energy were made with the linear accelerator of Kyoto University Research Reactor Institute). An absorber assembly was attached to the outside of the straight window of the scattering chamber, being insulated with Plexiglas plates. A thin collector, which was of the same material as the absorbers and put in an insulating sheath, was placed between the absorbers. Currents from the collector and the absorber assembly were respectively amplified with picoammeters, and then were fed to current integrators. Results obtained were given numerically in Ref. 5, in which comparisons were made with ETRAN Monte Carlo results of Berger and Seltzer obtained at slightly different energies. When the

comparisons were made in scaled coordinates of z/r_0 and r_0D_c (z denotes depth in the absorber; r_0 , the continuous slowing-down approximation range of electrons; and D_c , charge deposition per unit depth²) agreement between the experimental data and the ETRAN results were good except for the absorber of Be. ETRAN showed deeper average penetration for Be than experimental results.

Rogers later found that ETRAN showed deeper penetration than EGS Monte Carlo results in the calculation for the depth–dose curves of 1- to 50-MeV electrons incident on a water phantom [14]. Using a mixed-procedure Monte-Carlo code, Andreo and Brahme [15] found a similar discrepancy between the depth–dose curves obtained by them and by ETRAN for the central-axis depth–dose curve for 20-MeV electrons. Rogers and Bielajew [16] pointed out that the discrepancies were due to an error in the energy-loss straggling distribution used in ETRAN, i.e., the Landau distribution as modified by Blunck and Leisegang. Rogers and Bielajew wrote that because ETRAN had rightly been considered the definitive electron Monte Carlo transport code for over twenty years, their conclusions were somewhat surprising and demanded an answer to the question why this had not been *discovered* before. In fact, however, the present author’s group had discovered the discrepancies 15 years before from the comparison of the charge deposition profiles for Be.

Then Berger and Seltzer corrected the error in the sampling of the energy-loss straggling distribution in ETRAN, and the corrected version of ETRAN was incorporated into ITS. The present author’s group compared charge deposition profiles obtained by ITS as a byproduct of generating depth–dose curves with the earlier experimental results, and found that the discrepancies were removed [17]. To make better comparison, the present author’s group accurately interpolated the experimental results and obtained benchmark data on the charge deposition profile as well as on the derived parameters of the extrapolated range, most probable depth of charge deposition and average depth of charge deposition [6]. Comparisons of the interpolated experimental data on charge deposition profile with the ITS results generally showed good agreement. However, very small but systematic discrepancies were observed for the Au absorber. These discrepancies are numerically clear in the comparison of the average depth of charge deposition as shown in Table 1. The reason for these discrepancies is yet to be found.

Table 1. Relative deviations of ITS results of average depth of charge deposition from experimental data (cited from Ref. 6).

Incident energy of electrons	Relative deviation of ITS results from experiment in %
5 MeV	–3.6
10 MeV	–1.8
20 MeV	–2.5
Error in experimental results	± 1.3

² These are the notations of our later paper [6]. In the original paper [5], x , L and y_0 were used.